Int. J. Electrochem. Sci., 13 **(2018)** 8260 – 8274, doi: 10.20964/2018.08.120

International Journal of
ELECTROCHEMICAL
SCIENCE
www.electrochemsci.org

Dual-signal Amplification Strategy Aptasensor Based on Exonuclease III and Ordered Mesoporous Carbon-Gold Nanocomposites for Tetracycline Detection in Milk

Zengning Liu[#1,2], *Qingcui Xu*[#1,2], *Jiayun Fu*[1,2], *Zhaoqiang Shi*[1,2], *Qingqing Yang*[1,2], *Yemin Guo*[1,2,*], *Yanyan Zhang*[1,2], *Xia Sun*[1,2,*], *Zhiqiang Wang*[2,3]

[1] School of Agriculture Engineering and Food Science, Shandong University of Technology, No.12 Zhangzhou Road, Zibo 255049, Shandong Province, P.R. China
[2] Shandong Provincial Engineering Research Center of Vegetable Safety and Quality Traceability, No. 12 Zhangzhou Road, Zibo 255049, Shandong Province, P.R. China
[3] College of computer science and technology, Shandong University of Technology, No.12 Zhangzhou Road, Zibo 255049, Shandong Province, P.R. China
[*]E-mail: gym@sdut.edu.cn, sunxia2151@sina.com
#These authors contributed equally to this study.

Received: 7 May 2018 / *Accepted:* 23 June 2018 / *Published:* 5 July 2018

In this paper, a screen-printed aptasensor based on a dual-signal amplification strategy with enzyme-assisted target circulation and modification with ordered mesoporous carbon (OMC)-gold nanoparticle (AuNP) nanocomposites was used to detect tetracycline (TET) in milk. Exonuclease III (Exo III), an enzyme, is known to recognize double-stranded DNA nonspecifically. To take advantage of this intrinsic property, Exo III was selected to facilitate the target circulation and amplify the signal. Furthermore, OMC and AuNP nanocomposites formed a unique sensing film with a large surface area and good electronic conductivity, amplifying the current signal for tetracycline detection with excellent sensitivity. A TET-binding aptamer was self-assembled onto the surface of screen-printed carbon electrodes (SPCEs) modified with the nanocomposites to form a sensing layer. Additionally, Exo III sheared the hybridized double chain selectively, releasing the tetracycline target. The released target and the remaining hairpin probe hybridized again. After each cycle of digestion, the target was recycled, leading to amplification. Moreover, real milk samples were directly measured after diluting the milk 3 times. The results showed that the present dual-signal amplification strategy for tetracycline analysis exhibited a detection limit of 3.0 μg/L with high specificity and demonstrated its applicability for detecting tetracycline residues in milk samples.

Keywords: Aptasensor; Screen-printed carbon electrodes; Ordered mesoporous carbon; Tetracycline residues; Real-time field detection

1. INTRODUCTION

The antibiotic tetracycline (TET) is widely used to cure animal diseases, and the long-term application of subclinical doses in animal feed is used to prevent diseases in animals and to promote animal growth [1-2]. However, the continuous use of TET in animal feed has become a serious problem and may pose many risks to human health, such as permanent teeth yellowing, enamel dysplasia and bone growth inhibition [3-5]. For instance, excessive use of TET in dairy farming will lead to residual TET in milk and thus endanger consumer health.

In an effort to ensure food safety and human health, sensitive and fast methods for detecting residual TET in milk are needed. Over the last few years, many methods have been used to detect antibiotic residues, with the main methods being gas chromatography (GC), high-performance liquid chromatography (HPLC) [6-8] and immunoassays [9]. These sensitive and accurate methods can satisfy the requirements for detecting antibiotics. However, due to the disadvantages associated with these methods, including complexity, high cost, and time-consuming processes, the demand for simpler and more cost-effective methods has increased. Aptasensors can reduce the time and cost of analysis by simplifying or eliminating sample preparation, overcoming the limitations of the current analytical methods.

Currently, aptasensing methods are effective at detecting TET with better sensitivity than traditional methods. The detection of TET by aptasensors has become a developing trend in TET residue detection technology. Compared to antibodies, aptamers, which are also called artificial antibodies, exhibit many unique advantages, such as cost effectiveness, a reproducible synthesis process and a stable nature for continued target detection [10-12]. All kinds of methods using aptamer-based sensors, such as optical, enzyme, chromatographic, electrochemical and fluorescence methods, have been broadly used in the detection of TET [13]. Recently, many aptasensor for TET detection have been constructed by utilizing the specific reactions between aptamers and their targets. Aptasensors still have many problems, such as a low accuracy and a tedious pretreatment process; these problems make aptasensors unsuitable for field inspections. To overcome these problems, an enzyme was introduced in this work, and the pretreatment process was simplified.

In addition, electrode modification to amplify the signal is a critical factor for the preparation of aptasensors. As a nonsilicon mesoporous material with a large specific surface area and large aperture, ordered mesoporous carbon (OMC) has been widely used for developing biosensors located in various electron transfer mediators. In addition, ordered mesoporous carbon has good biocompatibility, conductivity and adsorbability compared with those of other mesoporous materials [14-16]. Gold nanoparticles (AuNPs) can effectively increase the electrical signal at the same time [17-19]; the gold sulfur bond in self-assembled films based on gold nanoparticles enables aptamers to be immobilized on the electrode surface better [20], effectively improving the stability of the aptasensor via the aptamer immobilization method.

A specific sequence is not strictly required for exonuclease III (Exo III) to recognize double-stranded DNA [21]. Because of this characteristic, Exo III was selected for the auxiliary target signal amplification cycle. The hairpin aptamer probe and the target TET on the surface of SPCEs will be hybridized, and Exo III will shear the hybridized double chain selectively, releasing the TET target

[22-24]. The released target and the rest of the hairpin probe will be hybridized again. In the presence of exonuclease, aptamer probes will be sheared again; after several cycles, some of the target will be released from the electrode surface, and the current signal will be increased significantly.

As mentioned above, Exo III was selected to facilitate the target circulation and amplify the signal. At the same time, OMC and AuNP nanocomposites can form a unique sensing film with excellent biocompatibility and electronic conductivity and an increased current signal for TET detection with excellent sensitivity. Moreover, in this experiment, real milk samples were directly measured by diluting the samples 3 times [25]. The results for the actual milk samples showed that the present dual-signal amplification strategy for TET analysis with this preprocessing method was feasible and sensitive. In combination with portable screen-printed carbon electrodes, this method provides a new approach for real-time detection of TET residues in the field.

2. EXPERIMENTAL

2.1 Apparatus

Electrochemical experiments were performed on a CHI660D electrochemical workstation (Shanghai Chenhua Co., China). A scanning electron microscope (SEM, Netherlands) was used to observe the morphologies of the modified electrodes. A three-electrode system was used at room temperature, and the working electrode was a TE100 screen-printed carbon electrode (SPCE) (d = 3 mm) obtained from Zensor R&D (Taiwan). An FE 20K Mettler-Toledo pH meter (Switzerland) was used to measure the solution pH values. Ultrasonication was performed with an SK3300H ultrasonic cleaner (Shanghai, China). A PTR-35 SPC vortex mixer (Britain) was used to mix the solution.

2.2 Reagents and materials

$NaH_2PO_4 \cdot 2H_2O$ and $Na_2HPO_4 \cdot 12H_2O$ were obtained from Beijing Chemical Technology Co., Ltd. (Beijing, China). A 0.1 M, pH 7.5 phosphate-buffer solution (PBS) was prepared using $NaH_2PO_4 \cdot 2H_2O$ and $Na_2HPO_4 \cdot 12H_2O$ mixtures. Ordered mesoporous carbon (OMC) was purchased from Nanjing Nanometer Technology Co., Ltd. (Nanjing, China). $K_3[Fe(CN)_6]$ and $K_4[Fe(CN)_6]$ were purchased from Yongda Chemical Reagent Co., Ltd. (Tianjin, China). Aptamers (Apt) specific for TET were purchased by Sangon Biotech Co., Ltd. (Shanghai, China) with the following DNA oligonucleotides [26]: 5'-SH-$(CH_2)_6$-CGT ACG GAA TTC GCT AGC CCC CCG GCA GGC CAC GGC TTG GGT TGG TCC CAC TGC GCG TGG ATC CGA GCT CCA CGT G-3'. TET was purchased from the Sigma (USA). All other reagents were analytical-grade reagents. All solutions were prepared using ultrapure water (18.2 MΩ·cm) and were purified by a Milli-Q purification system (Branstead, USA).

2.3. Preparation of ordered mesoporous carbon-chitosan (OMC-CS) composites

In total, 0.1 g of chitosan was dissolved in 100 mL of 1.0% acetic acid with 4 h of stirring to prepare a 0.1% (w/v) chitosan (CS) solution. Next, 1 mg of mesoporous carbon powder was dissolved in 4 mL of the chitosan solution, ultrasonicated for 30 min, and then placed on a programmed mixer for 30 min of shaking until the solution reached a uniform and stable state. The obtained highly dispersed black suspensions were 0.25 mg/mL mesoporous carbon chitosan composite solutions and were stored in a refrigerator at 4°C.

2.4. Preparation of gold nanoparticles (AuNPs)

Before the experiment, all glassware used was completely cleaned in aqua regia (3:1 mixture of HCl and HNO_3), then washed in triply distilled ultrapure water and dried in an oven. First, 100 mL of 0.01 wt% $HAuCl_4$ (w/v) aqueous solution in a flask was heated to boiling with uniform agitation. Then, 2.5 mL of 1% lemon acid sodium solution was rapidly added to the solution, which was boiled for 15 min with vigorous agitation. The solution was observed until the colour became ruby red. The solution was cooled to room temperature by effective agitation. The AuNPs [27] were successfully prepared and stored at 4°C.

2.5 Preparation of the hairpin aptamer

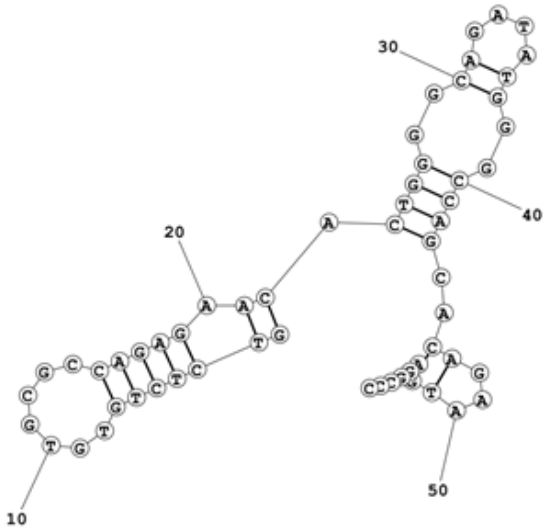

Figure 1. Hairpin structure of aptamer

The aptamer is a light dry film attached to the wall of the tube and is easily lost when the tube is opened. The tube should be centrifuged before the tube lid is opened, and then the tube cover should be opened slowly. According to the manual, to obtain a TET hairpin structure, a 100 M buffer can be prepared for each OD with 15 μL of buffer. To obtain a better hairpin structure, the storage solution was heated for 5 min in a water bath at 95°C and then slowly cooled to room temperature. Next, 150

μL of PBS (pH 7.2-7.4, 0.01 M) was added to each tube to prepare 10 M TET aptamer; after dissolving, the sample was stored at -20°C.

The hairpin structure of the aptamer is shown in Fig. 1.

2.6 Preparation of exonuclease III and the enzyme reaction system

The specification of Exo III is 4000 U, 20 L. To facilitate the modification of screen-printed carbon electrodes, we diluted the enzyme. The dilution solution contained 50 mM Tris-HCl, 50 mM KCl, and 1 mM DTT, and the enzyme was diluted to 1 U/μL. The enzyme reaction system was prepared as follows: $V_{\text{enzyme buffer}}:V_{\text{enzyme}}:V_{\text{PBS}} = 1:4:1$.

2.7 Preparation of an aptasensor based on a dual-signal amplification strategy

2.7.1 Preparation of SPCEs

Before the experiment, the bare SPCE was soaked in pH 5.0 PBS for 300 s and then subjected to a potential of +1.75 V. To obtain a steady-state current-voltage curve, the electrode was scanned at potentials ranging from +0.3 V to +1.25 V and -1.3 V to +0.3 V. All electrodes in the following experiments [28] were the pretreated SPCEs.

2.7.2 Preparation of TET/Exo III/BSA/Apt/AuNPs/OMC-CS/SPCEs aptasensor

For this step, 8 μL of mesoporous carbon chitosan nanocomposite was coated on the surface of the pretreated screen-printed carbon electrode and dried at room temperature to obtain OMC-CS/SPCEs. Then, 8 μL of gold nanoparticles was added to the surface of the modified electrode to obtain AuNPs/OMC-CS/SPCEs. Subsequently, the hairpin aptamer and BSA were dripped onto the electrode surface modified with the nanomaterials and dried at room temperature. Because the optimum temperature for the enzyme reaction was 37°C, 10 μL of the enzyme reaction system and target TET was added, and then the electrode was placed in a preheated electric baking oven. When the sample was dry, it was removed for testing.

2.7.3 Principle of enzyme-assisted target recycling

For Exo III, a specific sequence to recognize double-stranded DNA is not strictly required [29]. This experiment selected Exo III for the auxiliary target signal amplification cycle. When the TET target and hairpin aptamer hybridized, Exo III would selectively shear the hybridized product and then release of TET. The released TET and the rest of the hairpin aptamer probe will hybridize again. In the presence of Exo III, the aptamer probes will be sheared again, and after several cycles, a small amount of TET can be released from the surface of electrode, decreasing the obstacles for electrons and significantly increasing the current signal [30].

The experimental principle is shown in Fig. 2.

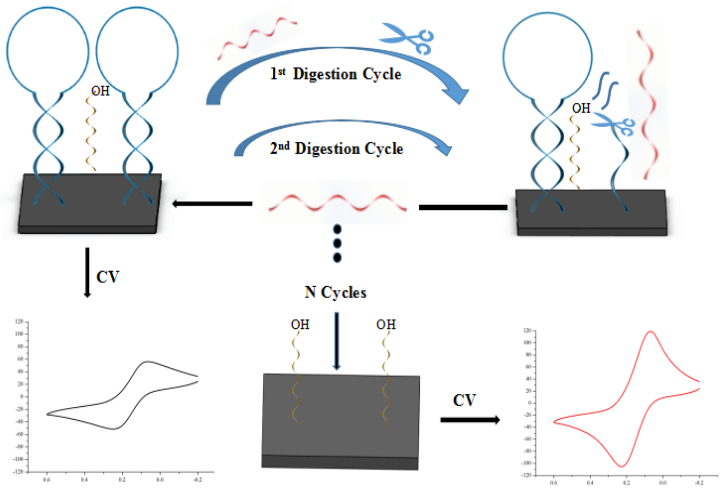

Figure 2. Schematic of cyclic amplification for enzyme assisted target cycling

2.7.4 Electrochemical measurements

Scanning electron microscopy (SEM) and CV were used to determine the properties of the nanomaterial modified on the electrode surface. The performance of these composites was tested in 15 mL of 0.1 M PBS (pH 7.0, with 5 mM $K_3Fe(CN)_6$]:$K_4[Fe(CN)_6$] =1:1 mixture as a redox probe and 0.1 M KCl) [31]. CV measurements were recorded from -0.2 to 0.6 V with a scan rate of 50 mV/s. The electrochemical differential pulse voltammetry (DPV) measurements were carried out with potentials ranging from -0.05 V to 0.4 V, a pulse height of 50 mV, a step height of 4 mV and a frequency of 15 Hz [32] to evaluate the sensitivity and specificity of the proposed aptasensor. In addition, the optimized aptasensor was used to detect TET by optimizing the parameters affecting the aptasensor response, such as pH of the PBS, the concentration of the aptamer and the loading of Exo III.

3. RESULTS AND DISCUSSION

3.1 SEM characterizations of modified electrodes

Scanning electron microscopy revealed the surface characteristics and structure of the prepared products. Fig. 3A shows the morphology of the gold nanoparticles, for which the distribution is uniform and compact and the surface area is large. Fig. 3B shows the morphology of the well-combined aptamer and gold nanoparticles. As shown in Fig. 3C, TET and the aptamer were combined in spirals with layers, and the structure was stable.

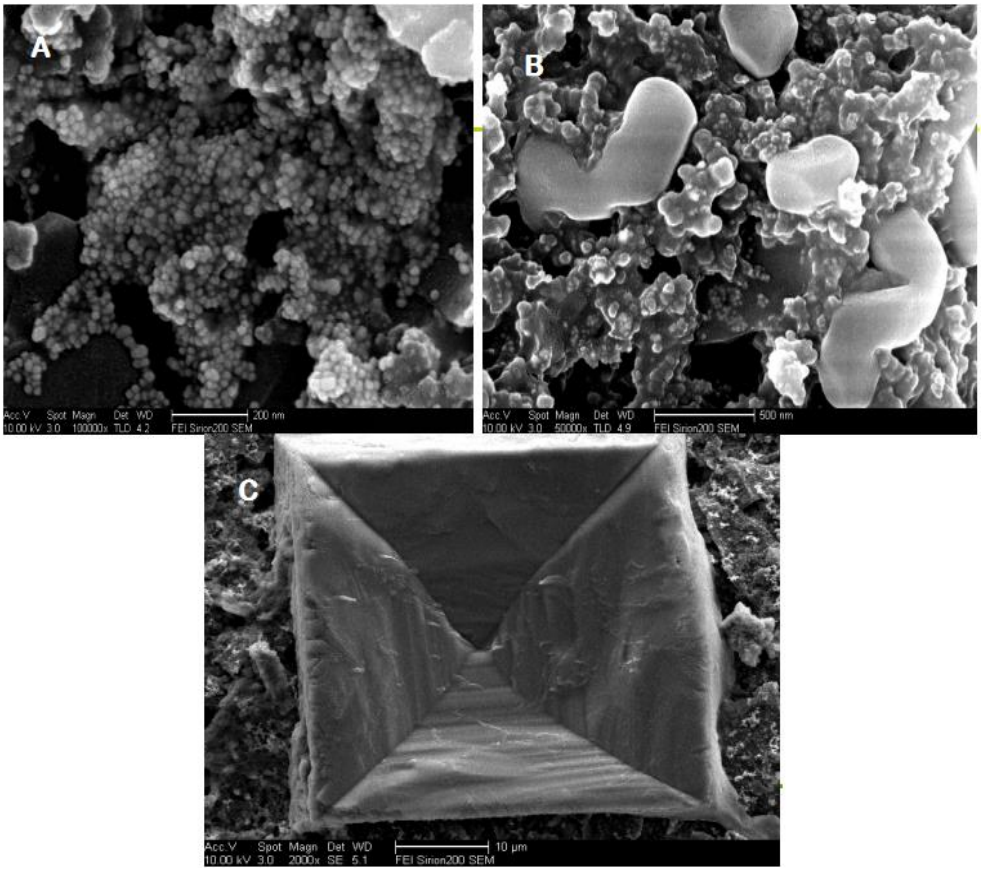

Figure 3. SEM image of (A): AuNPs; (B) : AuNPs-Apt; (C) : Apt-TET

3.2 Cyclic voltammetry characterization of the modified electrodes

The assembly process of the aptasensor was characterized by cyclic voltammetry (the bottom liquid contains 5 mM $[Fe(CN)_6]^{3-/4-}$ and 0.1 M KCl). The redox peaks of bare screen-printed carbon electrodes were clear, as shown in Fig. 4. OMC has good conductivity. The peak of the current increased significantly to 115.5 μA (curve b) after the OMC modification of the electrode. The AuNPs had good electrical conduction and a large surface area, and the peak current of AuNPs/OMC-CS/SPCEs was further increased to 133.5 μA (curve c). The peak current of the bare screen-printed carbon electrode was compared with that of OMC-CS/SPCEs electrode, and the peak of the AuNPs/OMC-CS/SPCEs further increased, indicating that OMC and AuNPs have synergistic effects (large surface area and good electrical conductivity). When the hairpin structure of aptamers and BSA was added to the electrode modified with nanomaterials, the structure of the hairpin aptamer exerted a large steric effect that spatially hindered the electron transfer between the $[Fe(CN)_6]^{3-/4-}$ solution and the electrode, and the negatively charged hairpin aptamer will prevent the $[Fe(CN)_6]^{3-/4-}$ solution and electrode from being close to each other. BSA can block specific sites on the surface of electrode, eliminating nonspecific binding, and BSA is a nonconductive protein so the electron transfer will be further hindered, thus leading to the rapid decrease in the peak current. This finding also demonstrated that the aptamer had been successfully fixed on the electrode surface (curve d). This result was consistent with that found in the literature [32-33].

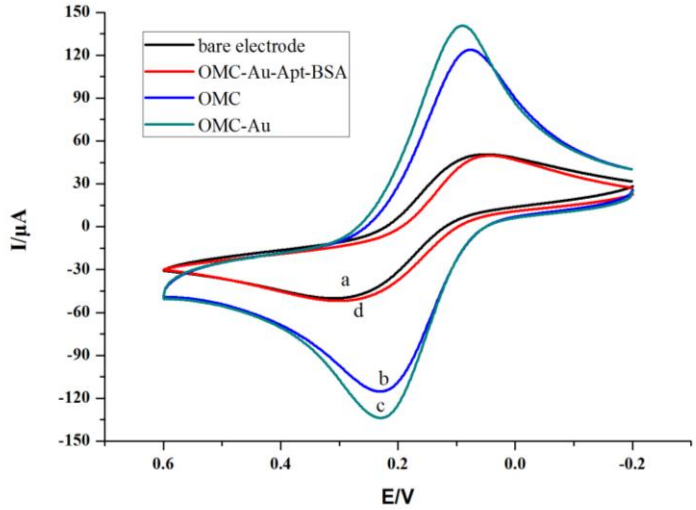

Figure 4. CVs of modified screen-printed carbon electrodes: (a) bare SPCEs; (b) OMC-CS/SPCEs; (c) AuNPs/OMC-CS/SPCEs; (d) BSA/Apt/AuNPs/OMC-CS/SPCEs

3.3 Signal test of the modified electrodes

To verify the ability of the enzyme-assisted target loop to amplify the signal, the aptasensor was compared with a conventional combination of aptamers and targets, as shown in Fig. 5.

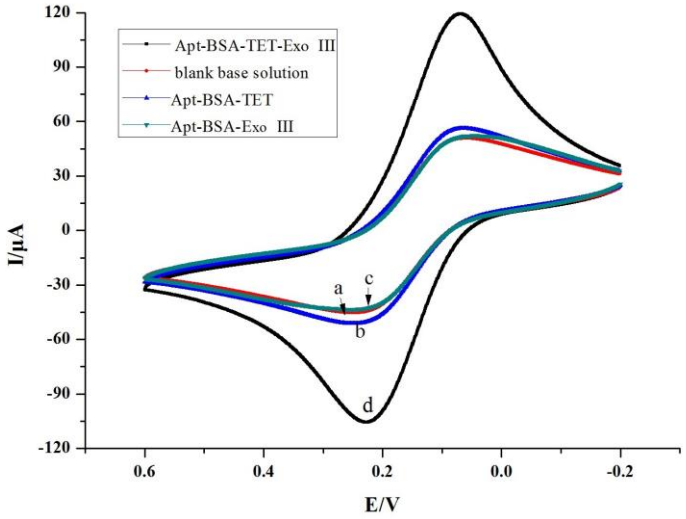

Figure 5. Signal test of aptasensor: (a) blank base solution; (b) Apt-BSA-TET; (c) Apt-BSA- Exo III; (d) Apt-BSA-TET-Exo III

In Fig. 5, curve a shows the CV measurements after the electrode was modified with the hairpin aptamer-BSA complex, which was considered the control sample. After 200 ng/mL TET was added , the peak current increased to 51.81 μA (curve b) because TET and the aptamer were combined

and the steric effect decreased, but the current changes were small. When TET was not present and the sample contained only Exo III, the current changes are very small compared with those of the control test; the decreases were only 1.7 μA (curve c). Then, TET was added during the addition of the enzyme reaction system, and the peak current increased significantly to 105.8 μA (curve d). Because of exonuclease III cutting that occurred when it combined with TET and the aptamer, a large part of the hairpin aptamer probe was removed from the electrode surface, promoting electron transfer between the electrode and the bottom liquid, and the current signal was significantly enlarged. Similar practices and results can be found in the literature [34].

3.4 Optimization of the experiment parameters

The bottom liquid pH influences the hairpin aptamer configuration. The product of the aptamer and TET in strong acidic or alkaline conditions is prone to dissociation, and the pH will also affect the exonuclease activity, thereby affecting the accuracy and sensitivity of the aptasensor. A series of different pH values (6, 6.5, 7, 7.5, 8, 8.5) of the phosphate buffer was prepared with 0.1 M PBS (pH 7, containing 5 mM $K_3[Fe(CN)_6]/K_4[Fe(CN)_6]$ and 0.1 M KCl) for a test solution. Fig. 6 shows the DPV response current change trend of TET/Exo III/BSA/Apt/AuNPs/OMC-CS/SPCEs in different pH test solutions. As shown in Fig. 6, when the bottom liquid was acidic or alkaline, the difference between the current response changed but did not achieve the best results. At pH 7.5, the current change response reached the maximum, and the aptamer and enzyme had the best effect, so pH 7.5 was chosen for the base test solution for experiments.

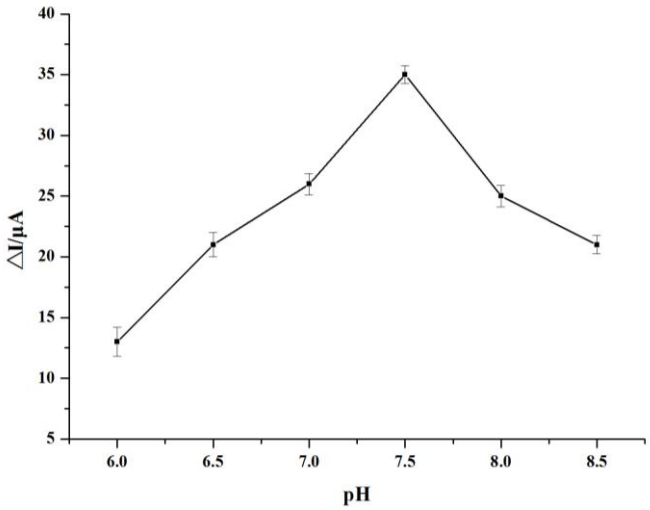

Figure 6. The optimum of the pH

The effect of the aptamer concentration on the performance of the aptasensor was also considered. Fig. 7 shows that with the increase in the aptamer concentration, the current difference increased gradually. In addition, when the concentration of aptamer reached 6 μM, the current

difference reached the maximum. Then, the response was almost constant as the aptamer concentration increased, indicating that the aptamer concentration immobilized on the electrode had reached the saturation concentration. Thus, the 6 μM aptamer concentration was employed to fabricate the aptasensor.

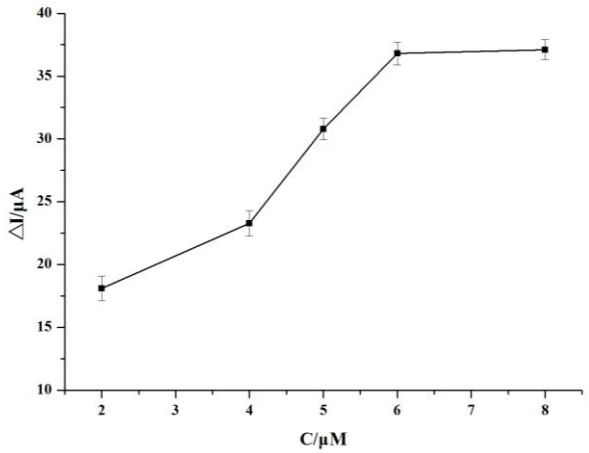

Figure 7. Optimization of aptamer concentration

The loading of Exo III also affected the biosensor current response. Fig. 8 shows the influence of Exo III immobilization on the response current of the TET/Exo III/BSA/Apt/AuNPs/OMC-CS/SPCEs sensor. As shown in the figure, as the loading of Exo III increased, the change in the current value increased at first and then slightly decreased, the amount of immobilized enzyme was 4 U, and the changes in the current response reached the maximum. The optimization trend of enzyme immobilization is the same as in the literature [35]. When the amount of enzyme immobilized was greater than 4 U, the change in the current value slightly increased, indicating that the amount of enzyme immobilized on the aptasensor had reached saturation. Therefore, in the follow-up, 4 U was selected for this component of the enzyme reaction system, and the enzyme was immobilized on the electrode surface.

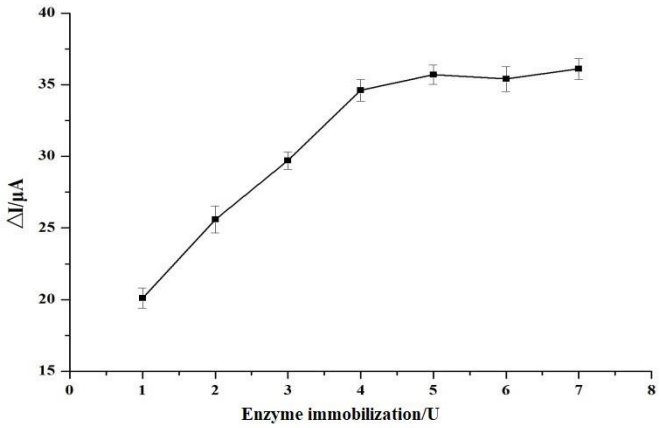

Figure 8. Optimization of the amount of enzyme immobilization

3.5 DPV response and calibration curve

The concentration of TET in an unknown solution was inferred from the relationship between the current response and the different aptasensor and TET concentrations. Fig. 9 shows the current changes for different concentrations of TET of TET/Exo III/BSA/Apt/AuNPs/OMC-CS/SPCE aptasensor. The difference in the current response also increased as the tetracycline concentration increased.

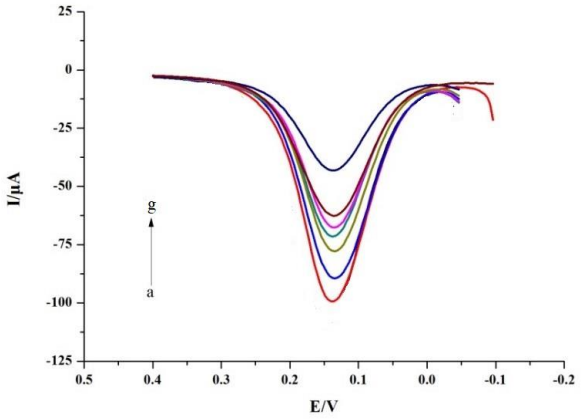

Figure 9. Relationship between current change and TET concentrations:(a) 1×103μg/L; (b) 1×102μg/L; (c) 10μg/L; (d) 1μg/L; (e) 10-1μg/L;(f) 10-2μg/L; (g) 10-3μg/L

As shown in Fig. 10, there was a good linear relationship between the current variation and the concentration of TET. Under the optimum conditions, the linear equation of TET in the range of 10^{-3} to 10^{3} g/L was y = 113.81669+8.3187x (R^2=0.9695), and detection limit was 0.03 g/L (S/N=3).

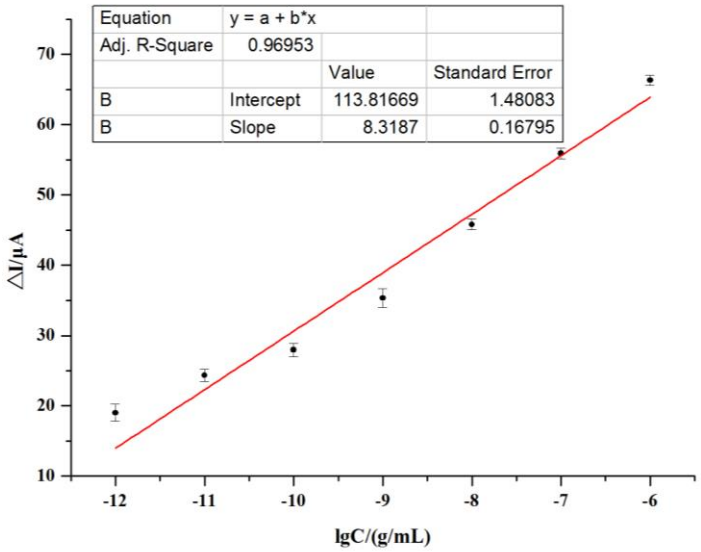

Figure 10. Relationship between current change and TET concentrations

3.6 Measurement of tetracycline in real samples

To further verify the performance of the prepared aptasensor, its applicability for detecting real samples, and the portability of screen-printed carbon electrode processing, a real-time detection method for direct dilution of the sample was performed to achieve field detection.

Dilutions of milk samples containing TET were varied at different times. When milk and buffer in a 1:1 ratio (milk:PBS=1:1) was used as the sample, the DPV curve was not smooth and had irregular changes (Fig. 11), illustrating that the matrix in milk had a great influence on the current response. When the milk sample was diluted 2 times or more, the matrix in milk may also still affect the current response, but the DPV curve was smooth. According to the stability of the current response of the milk for the various numbers of dilutions, the milk sample diluted 3 times was selected as the detection sample.

According to the results for the pretreatment step of milk dilution, milk that was diluted 3 times was chosen as the sample for recovery. To evaluate the influence of the matrix on the current response of the actual test samples, samples prepared in the same circumstances but with other assembly steps, such as eliminating the addition of TET to milk and the replacement of milk with two other solvents, were measured. The results showed the effect of the matrix in milk, which decreased the current response by 10 μA under the same conditions. The TET concentrations were 5×10^{-9} g/mL, 5×10^{-8} g/mL, and 5×10^{-7} g/mL. The above optimal conditions were used. The test results are shown in Table 1, and the recovery rate of the sample in the actual milk sample was 95.75-100.62%, which is within the allowable range of recovery. Additionally, as shown in Table 2, compared with other reported aptamers, the TET/Exo III/BSA/Apt/AuNPs/OMC-CS/SPCEs sensor had a lower detection limit and excellent sensitivity. These results showed that the aptasensor can be used for the rapid detection of TET residues in milk.

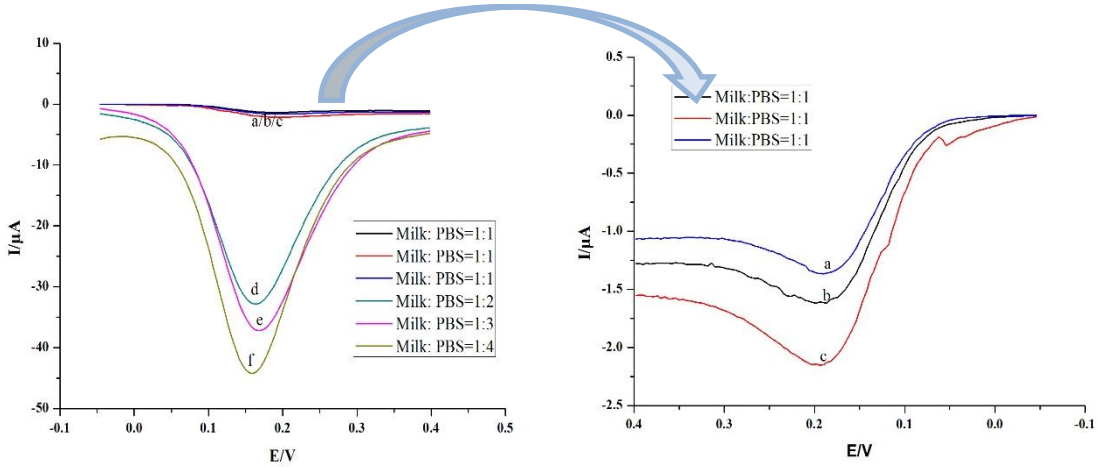

Figure 11. DPVs of diluted milk

Table 1. The recovery of the proposed aptasensor in real samples

Milk samples	Added (g/mL)	Standard value (△I/μA)	Detection value (△I/μA)	Recovery (%)	RSD (%)
1	5×10^{-9}	44.763	44.42	99.23	6.2
2	5×10^{-8}	53.082	53.41	100.62	4.3
3	5×10^{-7}	61.401	58.79	95.75	4.7

Table 2. Comparison of the response of the fabricated aptasensor with other aptasensor for detection of TET

Detection Sample	Nanoparticles involve in dection	LOD μ g/L	Detection technique	References
Milk	Multi walled carbon nanotubes	2.2	CV and DPV	36
Milk	AuNPs	39	Cysteamine-stabilized-AuNPs	37
Honey	AuNPs	12.4	Salt induction	38
Buffer	AuNPs	11.525	Salt induction	39
Milk	Exonuclease III and Ordered Mesoporous Carbon-Gold Nanocomposites	3.0	CV and DPV	This experiment

4. CONCLUSIONS

In conclusion, ordered mesoporous carbon and gold nanoparticles had a synergistic effect on electron transfer to amplify the aptasensor signal. At the same time, exonuclease III sheared the hybridized double-stranded region selectively, releasing the tetracycline target. The released target and the remaining hairpin probes hybridized again. After each cycle of digestion, the target was recycled, leading to amplification. Thus, a dual-signal amplification strategy aptasensor was designed based on exonuclease III and ordered mesoporous carbon-gold nanocomposites for tetracycline detection, and this aptasensor was successfully used for tetracycline detection in milk. Additionally, the pretreatment method of direct dilution was used for milk samples. The results showed that the method was practical and that tetracycline had a good linear relationship with the signal. In combination with the portability of screen-printed carbon electrodes, this method provided a new approach for real-time detection of tetracycline residues in the field.

ACKNOWLEDGMENTS
This work was supported by the National Natural Science Foundation of China (No.31471641, 31772068, 31701681), Special Project of Independent Innovation of Shandong Province

(2014CGZH0703), Shandong Provincial Natural Science Foundation (ZR2014CM009, ZR2015CM016, ZR2016CM29, ZR2017BC001, ZR2014FL003), Key Research and Invention Program of Shandong Province (2017GNC10119), Key Innovative project for 2017 Major Agriculture Application Technology of Shandong Province.

References

1. J. Guo, C.F. Zhang, G.Q. Gao, *Chinese J. Anim. Vet Adv.*, 41 (2014) 236.
2. Q.C. Xu, Z.N. Liu, J.F Fu, W.P. Zhao, Y.M Guo, X. Sun, H.Y. Zhang, *Sci.entific Rre.ports,* 7 (1) (2017) 14729.
3. M.X. Feng, G.N. Wang, K. Yang, H.Z. Liu, J.P. Wang, *Food Control*, 69 (2016) 171.
4. Q.C. Xu, Q.Q. Zhang, X. Sun, Y.M. Guo, X.Y. Wang, *RSC Adv.*, 6(21), 17328..
5. Q. Ouyang, Y. Liu, Q. Chen, Z. Guo, J. Zhao, H. Li, W. Hu, *Food Control*, 81 (2017) 156.
6. S. Liu, Z. Zheng, F. Wei, Y. Ren, W. Gui, H. Wu, G. Zhu, *J. Agric. Food Chem.*, 58 (2010) 3271.
7. W. Xie, C. Han, Y. Qian, H. Ding, X. Chen, *J. Chromatogr. A*, 1218 (2011) 4426.
8. F. Ma, C. Ho, A.K.H. Cheng, H.Z. Yu, *Electrochim. Acta.*, 110 (2013) 139.
9. Y.Q. Chen, Q. Chen, M. Han, J.Y. Liu, P. Zhao, L, D. He, Y. Zhang, Y.M. Niu, W.J. Yang, LY. Zhang, *Biosens. Bioelectron.*, 79 (2016) 430.
10. J. Tang, T. Yu, L. Guo, J. Xie, N. Shao, Z. He, *Biosens. Bioelectron.*, 22 (11) (2007) 2456.
11. Y. Wang, Z.H. Li, T.J. Weber, D.H Hu, C.T. Lin, J.H. Li, Y.H. Lin, *Anal. Chem.*, 85 (14) (2013) 67.
12. Y. Lian, F. He, H. Wang, F. Tong, *Biosens. Bioelectron.*, 65 (2015) 314.
13. L. Zhou, J. Wang, D. Li, Y. Li, *Food Chem.*, 162 (2014) 34.
14. X. Xu, M. Guo, P. Lu, R. Wang, *Mater. Sci. Eng.*, C 30 (2010) 722.
15. E. Ghasemi, E. Shams, N.F. Nejad, *J. Electroanal. Chem.*, 752 (2015) 60.
16. S.Y. Xu, X.Z. Han, *Biosens. Bioelectron.*, 19 (9) (2014) 1117.
17. M.T. Castañeda, S. Alegret, A. Merkoçi, Electroanalysis., 19 (7-8) (2010) 743.
18. M. Zhang, R. Yuan, Y. Chai, S. Chen, H. Zhong, C. Wang, Y.F. Cheng, *Biosens. Bioelectron.*, 32 (1) (2012) 288.
19. N. Chanda, M.F. Hawthorne, *Proc. Natl. Acad. Sci. U.S.A.*107 (19) (2010) 8760.
20. L. Zhou, M.H Wang, J.P. Wang, Y.Z. Zhou, *Chinese J. Anal. Chem.* 39 (3) (2011) 432.
21. C.L.W Liu, *Changsha, Hunan University*, (2016).
22. Y.L. Huang, Z.F. Gao, H.Q. Luo, N.B. Li,. *Sens. Actuators, B*, 238 (2017) 1017.
23. Y. Sun, P. Peng, R. Guo, H.W.T. Li, *Biosens. Bioelectron.*, 104 (2018) 32.
24. Y. Zhao, R. Liu, W. Sun, L. Lv, Z. Guo, *Sens. Actuators, B*, 255 (2018) 1640.
25. J. Zhang, Wuxi, *Jiangnan University*, 2014.
26. A. Wochner, M. Menger, D. Orgel, B. Cech, M. Rimmele, V.A. Erdmann, J. Glökler, *Anal. Biochem.* , 373 (1) (2008) 34.
27. F. L. Li, Zibo, *Shandong University of Technology*, 2014.
28. J. Cai, D. Du, *J. Appl. Electrochem.*, 38 (9) (2008) 1217.
29. M. Yan, W. Bai, C. Zhu, Y. Huang, J. Yan, A.L. Chen, *Biosens. Bioelectron.*, 77 (2016) 613.
30. Y. Chen, *Chem. Sen.* 35(3) (2015) 16scs.
31. Y.C. Jiao, H.Y. Jia, Y.M. Guo, H.Y. Zhang, Z.Q Wang, X. Sun, J. Zhao, *RSC Adv.*, 6(63) (2016) 58541.
32. J. Li, J. Huang, X.H. Yang, Y.J. Yang, K. Quan, N.L. Xie, Y.N. Wu, C.B. Ma, K.M. Wang, *Talanta*, 183 (2018) 11.
33. Q.Q. Zhang, Q.C. Xu, Y.M. Guo, X. Sun, X.Y. Wang, *Rsc Adv.*, 6(29) (2016) 24698.
34. H. Yin, Z. Yang, B. Li, Y. Zhou, S. Ai, *Biosens. Bioelectron.*, 66 (2015) 266.

35. Y.L. Huang, Z.F. Gao, H.Q. Luo, N. B. Li, *Sens. Actuators, B*, 238 (2017) 1017.
36. L. Zhou, D. Li, L. Gai, J.P. Wang, Y.B. Li, *Food Chem.*, 162 (2014) 34.
37. Y.L. Luo, J.Y. Xu, Y. Li, H.T. Gao, J.J. Guo, F. Shen,C.Y. Sun, *Food Control*, 54 (2015) 7.
38. S. Wang, S. Gao, S. Sun, Y. Yang, Y. Zhang, J. Liu,. *RSC Adv.*, 6 (2016) 45645.
39. M. Babaei, S.H. Jalalian, H. Bakhtiari, M. Ramezani, K. Abnous, S.M. Taghdisi, *Aust. J. Chem.*, 70 (2017) 718.